Revision 1

Thermal diffusivities of $MgSiO_3$ and Al-bearing $MgSiO_3$ perovskites

KENJI OHTA,[1,*] TAKASHI YAGI,[2] AND KEI HIROSE[3]

[1]Center for Quantum Science and Technology under Extreme Conditions, Osaka University, Toyonaka, Osaka 560-8531, Japan
[2]National Metrology Institute of Japan, National Institute of Advanced Industrial Science and Technology, Tsukuba, Ibaraki 305-8563, Japan.
[3]Earth-Life Science Institute, Tokyo Institute of Technology, Meguro, Tokyo 152-8551, Japan.

*E-mail: ohta@hpr.osaka-u.ac.jp

ABSTRACT

Thermal diffusivities of $MgSiO_3$ perovskite (MgPv) and $MgSiO_3$ perovskite containing 2 wt% Al_2O_3 (Al-MgPv) were measured at ambient conditions using the micro-spot heating Ångström method. The obtained values of thermal diffusivities of MgPv and Al-MgPv are 2.6 ± 0.1 and 2.4 ± 0.1 mm^2/s, respectively. Present result for MgPv is much higher than previously reported value of 1.7 mm^2/s. Substitution of aluminum into MgPv has little effect on its thermal diffusivity at ambient conditions, and such impurity effect would remain insignificant at high pressures and high temperatures corresponding to the Earth's lower mantle.

Keywords: thermal diffusivity, thermal conductivity, $MgSiO_3$ perovskite (MgPv), Al-bearing $MgSiO_3$ perovskite (Al-MgPv)

INTRODUCTION

To understand the thermal structure and the thermal evolution of the Earth, it is indispensable to know the transport properties of the material that constitutes the interior of the Earth. Since $MgSiO_3$ perovskite (MgPv) with some amount of iron and aluminum is accepted to be a primary mineral in the Earth's lower mantle (e.g., Hirose

2002), thermophysical properties of the (Al,Fe)-bearing MgPv are of great importance to comprehend the heat transfer system in the deep mantle. Osako and Ito (1991) reported lattice thermal diffusivity (D) of MgPv to be 1.7 mm^2/s at ambient conditions, from which lattice thermal conductivity ($\kappa = D\rho C_p$, where ρ is density and C_p is specific heat at constant pressure) was calculated to be 5.1 W/m/K. However, as Hofmeister and Branlund (2007) claimed, the conventional Ångström method involving multiple physical contacts, which was employed in Osako and Ito (1991) often underestimates thermal diffusivity due to the contribution of the contact resistance between the sample and heater or thermocouple. Thus the value of thermal diffusivity of MgPv at ambient conditions needs revisit by using a contact free method.

Recent technical progress both in the experiment and the theoretical calculation enables us to reveal high pressure and high temperature behavior of lattice thermal diffusivity (and conductivity) of lower mantle minerals, $MgSiO_3$ perovskite and MgO periclase (de Koker 2010; Stackhouse et al. 2010; Tang and Dong 2010; Manthilake et al. 2011; Haigis et al. 2012; Ohta et al. 2012; Dekura et al. 2013). However, there is only one report regarding the effect of chemical impurity on the lattice conductivity of the lower mantle minerals (Manthilake et al. 2011). They reported dissolution of 3 mol% $FeSiO_3$ or 2 mol% Al_2O_3 into MgPv induces ~70% decrease of the thermal diffusivity at 26 GPa and 300 K, which seems to be the significant impurity effect on the diffusivity relative to other mantle minerals. Measurements of iron-bearing olivine and orthopyroxene have yielded only 8% reduction in conductivity in the presence of 10 mol% iron (Horai 1971). Enrichment in aluminum into magnesium silicate is expected to have a smaller effect on the diffusivity because of the similarity in atomic mass of aluminum to magnesium and silicon relative to iron. Here we report the thermal diffusivities of perovskites on $MgSiO_3$ end member composition and on its Al-bearing solid solution at ambient conditions determined by the micro-spot heating Ångström method that is a contact free technique. We found that thermal diffusivity of MgPv is 2.6 ± 0.1 mm^2/s, 50% higher than the value reported by Osako and Ito (1991), and there is no measurable difference between the diffusivities for MgPv and Al-MgPv with 2 wt% Al_2O_3 at ambient conditions.

EXPERIMENTAL METHODS

A polycrystalline sample of MgPv has been synthesized from orthoenstatite (En) at

25 GPa and 2073 K for 1 hour in a multi-anvil apparatus. Starting material of En + 2 wt% Al_2O_3 in a rhenium capsule was also converted to Al-MgPv sample at 23 GPa and 2273 K for 1 hour. The perovskite structure was confirmed by a combination of micro-focused (50-100 μm) X-ray diffraction measurements and Raman spectroscopy.

The micro-spot heating Ångström method was employed to measure the thermal diffusivities of those perovskites (Fig. 1). This is a contact-free technique, and thus we can eliminate the contribution of contact resistance. A pump laser beam (808 nm wavelength, 3.7-7.0 mW laser power, modulated frequency f of 4 kHz, and 15 μm in diameter) periodically heats a 100 nm-thick Mo film deposited on the polished samples. During steady state heating, the heat inside the sample hemispherically propagates from the heated spot and oscillated with the frequency f. The reflectivity of the Mo film changes with temperature (i.e., thermoreflectance effect) (Weaver et al. 1975; Wang et al. 2010). The thermoreflectance effect of the Mo film induced by the temperature oscillation was detected using a continuous probe laser (782 nm wavelength, 1.5 mW laser power, and 5 μm in diameter). The temperature phase (θ) is negatively proportional to the distance from the heated spot (r), and the thermal diffusivity (D) of the sample can be determined by the following equation,

$$\theta = -\sqrt{\frac{\pi f}{D}} r + A \qquad (1)$$

where A is a constant. The probe laser scanned the sample surface by a 1-μm step to obtain a θ map around the heated spot with an area of 80 μm^2.

Artificially synthesized materials often contain micro size cracks. Such discontinuities inside the material potentially lead underestimation of the thermophysical properties of a bulk sample. In order to inspect our samples for the cracks, we obtained a widely scanned temperature phase (θ) maps for samples using a lower modulation frequency of 172 Hz. For MgPv, some discontinuities of heat conduction were observed which were highlighted by white broken line (Fig. 2a). The highlighted areas were almost overlapped with the cracks in the sample surface (Fig. 2b). This result indicates that cracks inside the sample inhibit heat conduction. We avoided such cracks in samples for accurate thermal diffusivity measurements, using the widely scanned map as a reference.

It is well known that MgPv undergoes crystal to amorphous transition when heated above 400 K at atmospheric pressure (Durben and Wolf 1992). This is also true for

Al-MgPv (Liu et al. 1995). Since the temperature increase at the heated spot is estimated to be about 50 K, and the temperature drops rapidly as r increases, crystallinity of both MgPv and Al-MgPv should be kept during experiments. After the diffusivity measurements, we also confirmed the crystallinity of the samples by means of the Raman spectroscopy.

RESULTS AND DISCUSSION

We measured thermal diffusivity of the MgPv sample at four areas (Fig. 3a). The pump beam of 4 kHz modulations heated the center of each measurement area. The spherical distribution of the θ indicates that the measured area has no cracks and homogeneous thermal diffusivity (Fig. 3b). The θ was plotted against the distance from the heated spot (r) in all directions (Fig. 3c). The amplitude of temperature oscillation decays with increasing the r, resulting the scatter of the θ in the r larger than 20 μm. We fitted the Equation 1 to the data in the r range between 10 and 20 μm to calculate thermal diffusivity (yellow line in Fig. 3c). The obtained values of the diffusivity of MgPv in each measurement area are summarized in Table 1. Averaged value of thermal diffusivity of MgPv is 2.6 ± 0.1 mm^2/s, from which the thermal conductivity is evaluated to be 8.1 W/m/K combining the reported values of heat capacity and density of MgPv (Akaogi and Ito 1993; Fiquet et al. 2000).

The obtained thermal diffusivity of MgPv is 50% higher than that reported by Osako and Ito (1991). As shown in Figure 2, cracks in the sample lower its thermal diffusivity. Measured sample in Osako and Ito (1991) is a bulk sample with a cylindrical shape, which could have many micro cracks, leading to substantial phonon scattering at the cracks and a reduction in thermal diffusivity. In addition, Hofmeister and Branlund (2007) claimed that the conventional Ångström method for minerals often underestimates by about 20% due to interface resistance between the sample and the heater or thermocouple. On the other hand, our method is a contact free technique and enables us to select the measurement area with no cracks. Thus we can avoid underestimation of thermal diffusivity. We have measured thermal diffusivity of MgPv in a pressure range between 11 and 144 GPa and 300 K, and have revealed pressure dependence of the diffusivity of MgPv ($\partial(\ln D_{MgPv})/\partial P$) of 1.2%/GPa by fitting the obtained data (Ohta et al. 2012). Combining the present result for MgPv at 1 bar, $\partial(\ln D_{MgPv})/\partial P$ is updated to be 1.1%/GPa, which is almost same to that we have

132 determined before (Ohta et al. 2012).

133 We also conducted similar thermal diffusivity measurements on the Al-MgPv
134 sample (Fig. 4a). As well as the measurements for MgPv, we selected measurement
135 areas with no cracks and homogeneous diffusivity (Fig. 4b), and determined thermal
136 diffusivities of selected areas with fitting obtained data via Equation 1 (Fig. 4c and
137 Table 1). The averaged thermal diffusivity of Al-MgPv is 2.4 ± 0.1 mm^2/s, which is a
138 comparable value to that of MgPv within the experimental uncertainty. The present
139 results indicate that substitution of aluminum into MgPv has little effect to the thermal
140 diffusivity, contradictory to the results of Manthilake et al. (2011). Thermal diffusivity
141 of MgPv at 26 GPa determined by Manthilake et al. (2011) is quite higher than other
142 high-pressure data for MgPv (Ohta et al. 2012; Dekura et al. 2013). This possible
143 overestimation of the diffusivity on MgPv could induce an apparently large effect of Al
144 substitution on the diffusivity of MgPv.

145 The effect of scattering by solute aluminum on the lattice thermal conductivity of
146 MgPv can be estimated as follows (Klemens 1960; Padture and Klemens 1997):

147 $$\kappa = \kappa_i \left(\frac{\omega_0}{\omega_M} \right) \arctan\left(\frac{\omega_M}{\omega_0} \right) \quad (2)$$

148 with

149 $$\left(\frac{\omega_0}{\omega_M} \right)^2 = \frac{\chi T}{C(1-C)} \quad (3)$$

150 where ω_M is the phonon frequency corresponding to the maximum of the acoustic
151 branch of the phonon spectrum, ω_0 is that phonon frequency where the intrinsic mean
152 free path is equal to that due to solute atoms, χ is a constant, and C is the concentration
153 of the solute atoms. κ_i is the solid-solution thermal conductivity without the solute-atom
154 phonon scattering and is given by

155 $$\kappa_i = C\kappa_A + (1-C)\kappa_B \quad (4)$$

156 where κ_A and κ_B are the thermal conductivities of solids with end member compositions
157 of $C = 0$ and $C = 1$, respectively, at a given temperature. At high temperature conditions
158 corresponding to the lower mantle, as (ω_M/ω_0) is very small, $\arctan(\omega_M/\omega_0)$ will be
159 comparable to (ω_M/ω_0). Then, the scattering effect will be negligible at high temperature.
160 In addition, according to Hofmeister (1999), a pressure derivative of thermal
161 conductivity of Al_2O_3 corundum is similar to that of MgPv, and thus the difference in

the conductivity between MgPv and corundum will not change appreciably even at high pressures. Hence the lower mantle impurity effect of solute aluminum in silicate perovskite is predicted to be weak. The effect of iron on the conductivity of MgPv also needs to be investigated. Direct measurements of thermal diffusivity of (Mg,Fe)O ferropericlase, (Al,Fe)-bearing silicate perovskite, and post-perovskite under actual Earth's lower mantle condition will provide tighter constraints on thermal transport properties of Earth's mantle.

ACKNOWLEDGEMENTS

Comments from two anonymous reviewers were helpful to improve the manuscript. K.O. is supported by the Japan Society for Promotion of Science.

REFERENCE CITED

Akaogi, M., and Ito, E. (1993) Heat capacity of $MgSiO_3$ perovskite. Geophys. Res. Lett., 20, 105-108.

de Koker, N. (2010) Thermal conductivity of MgO periclase at high pressure: Implications for the D″ region. Earth Planet. Sci. Lett., 292, 392-398.

Dekura, H., Tsuchiya, T., and Tsuchiya, J. (2013) *Ab initio* lattice thermal conductivity of $MgSiO_3$ perovskite as found in Earth's lower mantle. Phys. Rev. Lett., 110, 025904.

Durben, D.J., and Wolf, G.H. (1992) High-temperature behavior of metastable $MgSiO_3$ perovskite: a Raman spectroscopic study. Am. Miner., 77, 890-893.

Fiquet, G., Dewaele, A., Andrault, D., Kunz, M., and Bihan, T. (2000) Thermoelastic properties and crystal structure of $MgSiO_3$ perovskite at lower mantle pressure and temperature conditions. Geophys. Res. Lett., 27, 21-24.

Haigis, V., Salanne, M., and Jahn, S. (2012) Thermal conductivity of MgO, $MgSiO_3$ perovskite and post-perovskite in the Earth's deep mantle. Earth Planet. Sci. Lett., 355-356, 102-108.

Hirose K. (2002) Phase transitions in pyrolitic mantle around 670-km depth: Implications for upwelling of plumes from the lower mantle. J. Geophys. Res., 107, 2078, 10.1029/2001JB000597.

Hofmeister, A.M. (1999) Mantle values of thermal conductivity and the geotherm from phonon lifetimes. Science, 283, 1699-1706.

Hofmeister, A.M., and Branlund, J.M. (2007) Properties of rocks and minerals- Thermal conductivity of the Earth. Treat. Geophys., 1, 543-577.

Horai, K. (1971) Thermal conductivity of rock-forming minerals. J. Geophys. Res., 76, 1278-1308.

Klemens, P. G. (1960) Thermal resistance due to point defects at high temperatures. Phys. Rev., 119, 507-509.

Liu, L., Mernagh, T.P., and Irifune, T. (1995) Raman spectra of $MgSiO_3$·10% Al_2O_3-perovskite at various pressures and temperatures. Phys. Chem. Miner., 22, 511-516.

Manthilake, G.M., de Koker, N., Frost, D.J., and McCammon, C.A. (2011) Lattice thermal conductivity of lower mantle minerals and heat flux from Earth's core. Proc. Natl. Acad. Sci. U.S.A., 108, 17901-17904.

Ohta, K., Yagi, T., Taketoshi, N., Hirose, K., Komabayashi, T., Baba, T., Ohishi, Y., and Hernlund, J. (2012) Lattice thermal conductivity of $MgSiO_3$ perovskite and post-perovskite at the core-mantle boundary. Earth Planet. Sci. Lett., 349-350, 109-115.

Osako, M., and Ito, E. (1991) Thermal diffusivity of $MgSiO_3$ perovskite. Geophys. Res. Lett., 18, 239-242.

Padture, N., and Klemens, P. (1997) Low thermal conductivity in garnets. J. Am. Ceram. Soc., 80, 1018-1020.

Stackhouse, S., Stixrude, L., and Karki, B. (2010) Thermal Conductivity of Periclase (MgO) from First Principles. Phys. Rev. Lett., 104, 208501.

Tang, X., and Dong, J. (2010) Lattice thermal conductivity of MgO at conditions of Earth's interior. Proc. Nat. Acad. Sci. USA, 107, 4539-4543.

Wang, Y., Park, J.-Y., Koh, Y.K., and Cahill, D.G. (2010) Thermoreflectance of metal transducers for time-domain thermoreflectance. J. Appl. Phys., 108, 043507.

Weaver, J.H., Olson, C.G., Lynch, D.W., Piancentini, M. (1975) Thermoreflectance of Mo from 0.5 to 35 eV. Solid State Comm., 16, 163-166.

FIGURE CAPTIONS

Figure 1. Schematic of thermal diffusivity measurement by the micro-spot heating Ångström method. Thermal diffusivity of the sample can be calculated by using Equation 1.

Figure 2. Photographs of the MgPv sample before Mo coating (a) with and (b) without a scanned temperature phase (θ) map. Areas with low θ almost overlap cracks in the sample indicated by white lines.

Figure 3. (a) Photograph of the MgPv sample before Mo coating. Four squares indicate measurement areas. (b) Distribution of the θ for the area 1 (yellow square in Fig. 2a). (c) The θ as a function of the distance from the heated spot (r) for the area 1. Thermal diffusivity of MgPv was calculated in the range of r between 10 and 20 μm (yellow line) by using Equation 1.

Figure 4. (a) Photograph of the Al-MgPv sample before Mo coating (Upper room of rhenium capsule). Yellow and blue squares are measurement areas. (b) Distribution of the θ for the area 1 (Yellow square in Fig. 4a). (c) The θ as a function of the r for the area 1. Yellow line shows a fitting range of r to calculate the diffusivity of Al-MgPv by using Equation 1.

TABLE 1. Thermal diffusivities of MgPv and Al-MgPv at each measurement point.

Sample	Measurement point	θ/r (rad/m)	Thermal diffusivity, D (mm^2/s)
MgPv	1	71600	2.45
	2	71300	2.47
	3	67900	2.73
	4	68200	2.70
Al-MgPv	1	71300	2.47
	2	74000	2.30

Modulation frequency (f) of the pump laser is 4 kHz.
The values of θ/r were derived from the data of r = 10 ~ 20 μm.
Thermal diffusivity (D) was calculated using Equation 1.

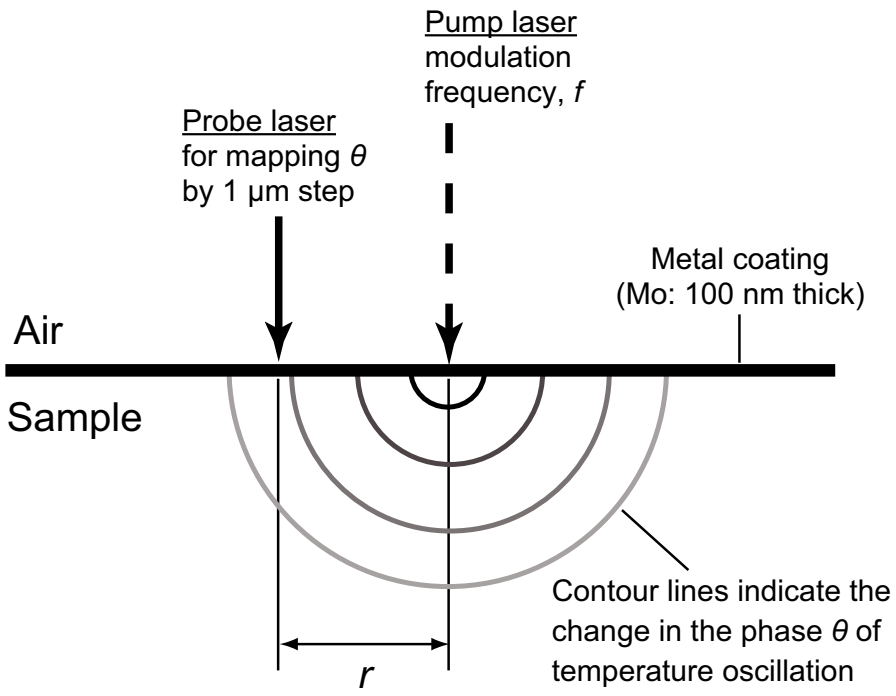
Pump laser
modulation
frequency, f
Probe laser
for mapping θ
by 1 μm step
Metal coating
(Mo: 100 nm thick)
Air
Sample
Contour lines indicate the
change in the phase θ of
temperature oscillation
r

FIGURE 1

(a)

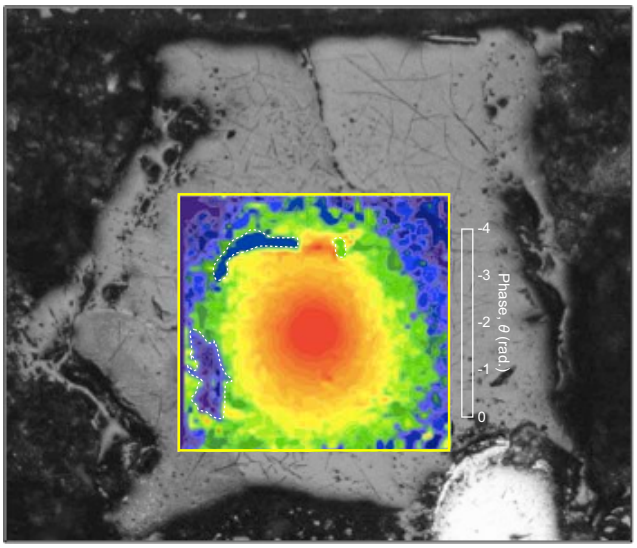

(b)

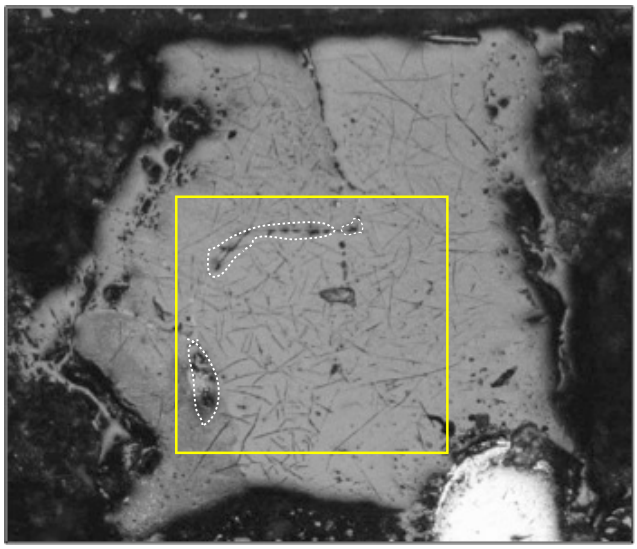

FIGURE 2

(a)

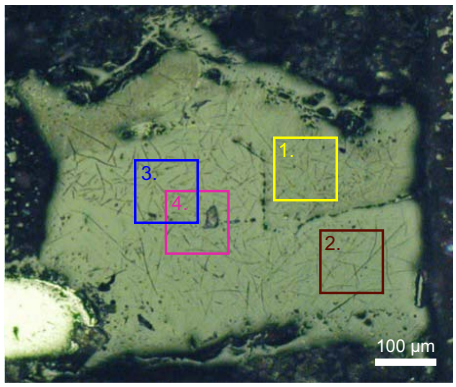
1.
2.
3.
4.
100 µm

(b)

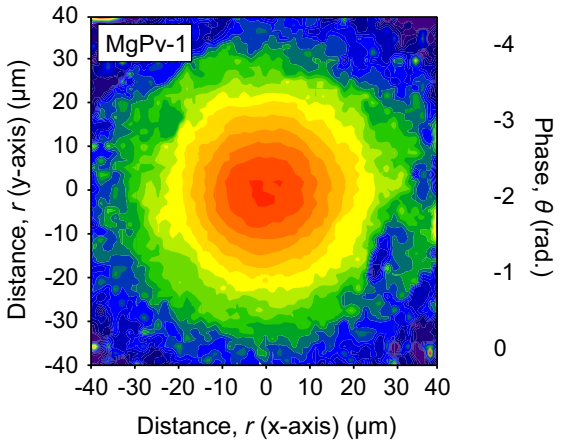
MgPv-1
Distance, r (y-axis) (µm)
Distance, r (x-axis) (µm)
Phase, θ (rad.)
40
30
20
10
0
-10
-20
-30
-40
-40 -30 -20 -10 0 10 20 30 40
-4
-3
-2
-1
0

(c)

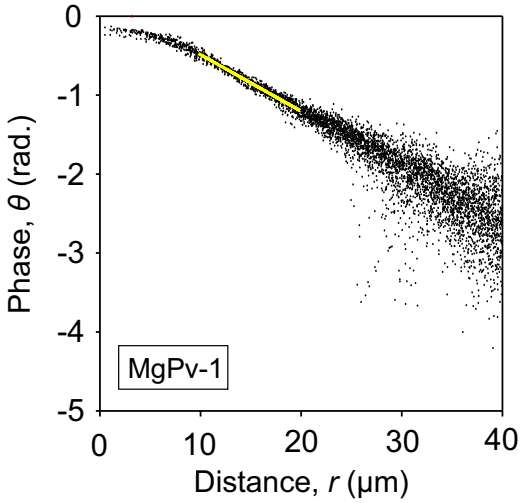
MgPv-1
Phase, θ (rad.)
Distance, r (µm)
0
-1
-2
-3
-4
-5
0 10 20 30 40

FIGURE 3

(a)

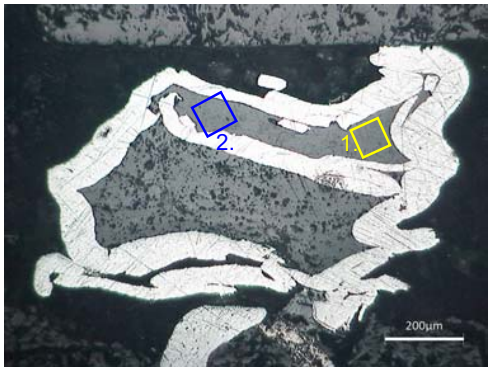
2.
1.
200μm

(b)

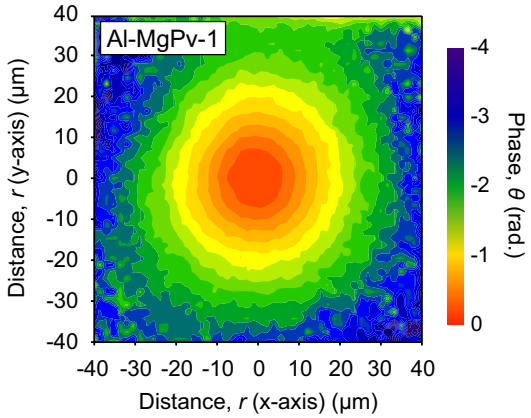
Al-MgPv-1
Distance, r (y-axis) (μm)
40
30
20
10
0
-10
-20
-30
-40
-40 -30 -20 -10 0 10 20 30 40
Distance, r (x-axis) (μm)
-4
-3
-2
-1
0
Phase, θ (rad.)

(c)

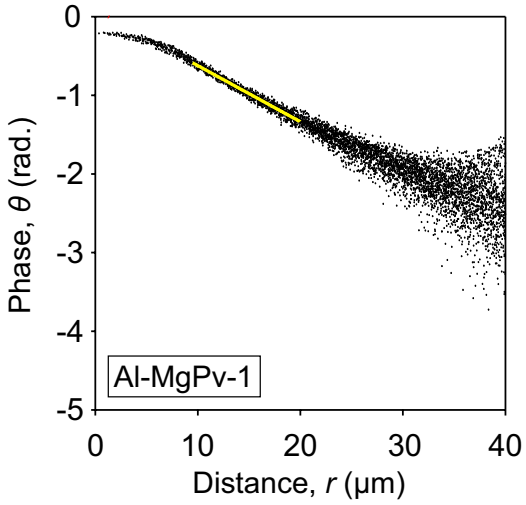
Phase, θ (rad.)
0
-1
-2
-3
-4
-5
Al-MgPv-1
0 10 20 30 40
Distance, r (μm)

FIGURE 4